

WATER SOLUTION POLISHING OF NITRATE USING POTASSIUM PERMANGANATE MODIFIED ZEOLITE: PARAMETRIC EXPERIMENTS, KINETICS AND EQUILIBRIUM ANALYSIS

MOHSENIBANDPEI A.¹

GHADERPOORI M.²

HASSANI G.^{3,4}

BAHRAMI H.⁵

BAHMANI Z.⁶

ALINEJAD A.A.^{5,*}

¹*Environmental and Occupational Hazards Control Research Center Shahid Beheshti University of Medical Sciences, Tehran, Iran*

²*Students Research committee*

Department of Environmental Health Engineering

Shahid Beheshti University of Medical Sciences, Tehran, Iran

³*Social Determinants of Health Research Center*

Yasuj University of Medical Sciences, Yasuj, Iran

⁴*Department of Environmental Health Engineering, Faculty of Health*

Yasuj University of Medical Sciences, Yasuj, Iran

⁵*Department of Environmental Health Engineering, School of Public Health*

Shahid Beheshti University of Medical Sciences, Tehran, Iran

⁶*Social Determinants in Health Promotion Research Center*

Hormozgan University of Medical Sciences, Bandar Abbas, Iran

Received: 13/11/2015

Accepted: 29/02/2016

Available online: 03/06/2016

*to whom all correspondence should be addressed:

e-mail: azimalinejad@gmail.com

ABSTRACT

In the present study, adsorption potential of potassium permanganate (Hypermangan) modified zeolite was investigated for the removal of nitrate from synthetic wastewater. Effects of the most significant parameters (pH, adsorbent dose, nitrate concentration and contact time) were initially evaluated based on the percentage of nitrate removed from the water solutions. Over 90 % removal of 150 mg l⁻¹ nitrate was achieved at an optimum pH of 5, adsorbent dose of 2g l⁻¹ after a 60 min contact time. The chemical and morphological characterizations of Hypermangan modified zeolite (HMZ) were carried out by using scanning electron microscopy (SEM), fourier transform infrared (FT-IR), x-ray diffraction (XRD) and x-ray fluorescence (XRF) analysis methods. Kinetic evaluation indicated that the nitrate adsorption onto HMZ followed the pseudo-first-order model. The equilibrium data assessment illustrated the removal of nitrate by HMZ follows a Langmuir model which attains the maximum adsorption capacity 6.7 mg g⁻¹. The mean free energy of adsorption was 0.15 kJ mol⁻¹, which indicates the adsorption of nitrate onto HMZ, occurs through a physical mechanism.

Keywords: Hypermangan, Nitrate, Adsorption, Equilibrium, Kinetic

1. Introduction

Pollution of water resources by nitrate occurs due to industrial wastewater containing nitrate, domestic wastewater, fertilizers in agricultural, discharges from animal operations, wastewater treatment facilities,

septic systems and commercial activities (Benyoucef *et al.*, 2013; Cheikh *et al.*, 2013). It causes eutrophication problems of rivers, lakes and seas, destroys water quality and presents potential hazards on human health. The WHO guideline value for nitrate is 50 mg l^{-1} (Cheikh *et al.*, 2013). It needs to be regulated in water basically because excess levels of nitrate effects on health by forming methemoglobinoma in children, hypertension, thyroid disability and carcinogenicity hazard of nitrosamine (Benyoucef *et al.*, 2013). Current nitrate removal techniques include ion exchange, biological denitrification, chemical treatment, reverse osmosis, electrodialysis, catalytic denitrification, membrane filtration, electrocoagulation and adsorption (Zhang *et al.*, 2009; Malekian *et al.*, 2011; Montalvo *et al.*, 2011; Andalib *et al.*, 2012; Rezakazemi *et al.*, 2012; Bravo *et al.*, 2013; Jiang *et al.*, 2013; Yu *et al.*, 2013). Among these methods, adsorption is generally considered to be a simple and efficient method for the removal of nitrate. With the advancement of nanotechnology, attempts have been made in the use of zeolites and their modification form such as hydrated aluminosilicate materials, bentonite and kaoline due to their low cost and availability in large amounts on the earth (Dong *et al.*, 2010; Gupta *et al.*, 2011). Nowadays because of the low cost and simplicity adsorbents such as natural and synthetic zeolite modified, activated carbon fibers and polymeric adsorbents are employed for sorption of pollutants (Gupta and Bhattacharyya, 2008; Hajdu *et al.*, 2012). Lately, several modification methods including hypermangan modification, iron modification, and lanthanum modification have attracted more notice due to improve the zeolite performance, e.g., adsorption capacity and increased mechanical, resistance to chemical environment, physical and chemical properties, high specific surface (surface to volume ratio) and high absorption efficiency. Therefore, in recent times, the interest in new type hypermangan-modified adsorbents is increasing with each passing day (Han *et al.*, 2006a; Han *et al.*, 2006b; Zou *et al.*, 2006; Al Ghouti *et al.*, 2009). In this study hypermangan modification is used due to microporous structure, high specific surface, high absorption efficiency, and lack of penetration resistance due to the elimination of the interior absorption surfaces in porous adsorbent, the possibility to modify and adjust the surface properties of hypermangan. The use of hypermangan adsorbent in form of powder has practical limitations, such as hardness solid/liquid separation, high pressure drop and leaching of metal/metal oxide in final treated water. Thus, to overcome these problems, hypermangan can be coated on zeolite surface to provide an effective adsorbent for nitrate removal from water. It appears that this method provides an effective surface and may increase the pollutants removal from water. The purpose of this study was to construct HMZ, for polishing of water solutions content nitrate that was carried out in batch laboratory system. The nitrate adsorption feasibility onto HMZ was examined by evaluating the effects of various operating conditions such as (pH, adsorbent dose, nitrate concentration and contact time). The chemical and morphological characterizations of HMZ were carried out by using SEM, FT-IR, XRD and XRF analysis methods.

2.1. Materials and methods

2.1.1. Materials

The natural zeolite with a grain size range 1-5 mm, supplied by a company in Semnan province, Iran. The chemical composition of Semnan zeolite is listed as follows, in mass %: MnO= 0.04, P₂O₅ = 0.01, SiO₂ = 66.5, Al₂O₃ = 11.81, Na₂O= 2.01, CaO = 3.11, MgO= 0.72, K₂O= 3.12, Fe₂O₃ = 1.3, TiO₂ =0.21 and loss of ignition (LOI) = 12.05 that were determined by XRF analysis. Prior to use, the natural zeolite was crushed and sieved to the average particle diameter. Then it was soaked in tap water for 24 h to decrease its alkaliness. Potassium permanganate (Sigma-Aldrich, USA) and HCl (Merck) were used to prepare the HMZ. A stock solution was prepared with dissolving 1.0 g of analytical grade potassium nitrate (KNO₃) in 1000 mL deionized water.

2.1.2. Preparation of potassium permanganate modified zeolite

In preparation for surface coating, zeolite sample was washed with deionized water and dried at 373 °K in the oven. The chemical precipitation used to make HMZ. The zeolite was converted to its Na form by suspending 50 g into 500 ml of a 2M NaCl solution for a period of 24 h. Then zeolite was washed with deionized water to remove chloride ions, and dried at room temperature. The zeolite was placed in beaker and a boiling solution

containing potassium permanganate was added into beaker over zeolite. The hydrochloric acid was added into beaker and the solution was mixed at 90 °C for 1 hours. The media was separated, washed with deionized water and dried at room temperature. It was stored in a polypropylene bottle for further use.

2.2. Characterization of Adsorbent

The powder x-ray diffraction (PXRD) technique using (PANalytical 3040/60 X, Pert PRO) with Cu K α radiation source over a range of 10-60 nm at a scan speed 1 s/step, 1.54 Å wavelength and 25 °C, was used to measure the crystallinity of samples and compound formation. Diffraction peaks were used to identify the structure of samples by matching their observed patterns with the standard pattern of zeolite (ICDD ASCII card No (01-087-2334)). Chemical composition of zeolite was measured by a Shimadzu XRF-1800 with Rh radiation. The Scanning electron micrograph (SEM) (Hitachi S-3000N, Japan) was applied to analyze the morphological structure and topological presentation of HMZ.

FTIR analysis was conducted in a WQF-510A/520A FTIR Spectrometer; the samples were prepared using the KBr pressed disk technique, with 1% inclusions of the sample to be analyzed. The zero point of charge for adsorbent was determined to investigate the surface charge of adsorbent material. To determine of p*H*_{ZPC}, 50 mL of potassium nitrate (0.01M) solution was added to Erlenmeyer flasks. Initial solution pH was adjusted between 2 to 12 by addition of HCl and NaOH. Then 0.2 g of adsorbent was added to the Erlenmeyer flasks and mixed for 24 h. Final pH of solution was measured by using a pH meter (model 50-pp-sartorius). Curve of initial pH versus final pH was plotted and the intersection point of curves was recorded as p*H*_{ZPC} (Nghah & Hanafiah 2008). The specific surface area (based on the BET method) and pore volume were determined by nitrogen gas adsorption analyzer (Micromeretics/Gemini-2372).

2.3. Experimental procedure

Batch experiments were carried out in conical flasks containing a definite volume (100 ml in each case) with a magnetic stirrer using a constant speed of 200 rpm. Stock solution of nitrate (1000 mg l⁻¹) was prepared and the desired concentrations of nitrate were obtained by diluting the stock solution. Table 1 presents experimental runs and conditions. For each experiment, 100 ml nitrate solution was added to the flask, and the test conditions were adjusted to the designated level (Table 1).

Table 1. Experimental runs and conditions for nitrate adsorption onto HMZ.

Run	Condition	Parameter			
		pH	Nitrate concentration (mg l ⁻¹)	HMZ dosage (g l ⁻¹)	Contact time (min)
1	The effect of pH	2-11	150	2	60
2	The effect of HMZ dosage	5	150	0.1-2.5	60
3	The effect of contact time	5	150	2	3-100
4	Equilibrium tests	5	100-300	2	60

After a certain period of time, solid–liquid separation was achieved by centrifugation at 3000 rpm (for 3 min). The final concentration of nitrate in the clear solution was determined according to method mentioned in the Standard Method at 220 nm, using a TU-1901 UV/vis spectrophotometer (Beijing Purkinje General Instrument Co., Ltd., China) (APHA, 2005). Each experiment was conducted three times.

2.4. Kinetic and isotherm analysis

To evaluate the isotherm models, 2 g HMZ was stirred in 100 mL of different concentrations of the solution (100-300 mg l⁻¹) at a pH of 5 for 60 min. In this study, the adsorption of nitrate from its aqueous solution by HMZ was investigated with four of the most used isotherm models (Langmuir, Freundlich, Temkin and (D-R)). The Langmuir, Freundlich, Temkin and D-R isotherm equations are stated as Eqs. 1-4:

$$\frac{C_e}{q_e} = \frac{1}{q_m b} + \frac{1}{q_m} C_e \quad (1)$$

$$\log q_e = \log k_f + \frac{1}{n} \log C_e \quad (2)$$

$$q_e = B \ln K_t + B \ln C_e \quad (3)$$

$$\ln q_e = \ln q_m - K_{DR} \epsilon^2 \quad (4)$$

Where C_e is the equilibrium concentration of adsorbate in solution [mg l^{-1}], q_e is the amount adsorbed of equilibrium [mg g^{-1}], q_m [the amount of ultimate adsorption capacity [mg g^{-1}]] and b [energy of adsorption [l mg^{-1}]] are the Langmuir constants that can be calculated from the slope and intercept of the linear plot of C_e versus C_e/q_e respectively. k_f and $1/n$ are the Freundlich constants related to adsorption capacity and adsorption intensity respectively, that can be obtained from the intercept and slope the linear plot of $\log q_e$ versus $\log C_e$. For a favorable adsorption n should have values lying in the range of 0 to 1. K_t is the equilibrium binding constant [l mg^{-1}] and B is the variation of adsorption energy [KJ mol^{-1}], K_t and B can be calculated from the slope and intercept the linear plot of q_e versus $\ln C_e$. K_{DR} is a constant related to mean free energy of sorption per mol of the sorbate [$\text{mg}^2 \text{kJ}^{-2}$] and ϵ is Polanyi potential [J mg^{-1}]. K_{DR} can be calculated from the slope of the linear plot of $\ln q_e$ versus ϵ^2 . Also ϵ can be obtained using following equation:

$$\epsilon = RT \ln \left(1 + \frac{1}{C_e} \right) \quad (5)$$

Where R is the universal gas constant [$8.314 \text{ KJ/kmol } ^\circ\text{K}$] and T [$^\circ\text{K}$] is the absolute temperature (Khorramfar *et al.*, 2009). The essential characteristics of Langmuir isotherm, commonly known as the separation factor or equilibrium parameter (R_L) is presented in Eq. (7).

$$R_L = \frac{1}{[1 + bC_0]} \quad (6)$$

The kinetics of adsorption was investigated by shaking 2 g HMZ in concentration 150 mg l^{-1} of nitrate at a pH of 5 and varying contact times (5-60 min). Adsorption kinetics of Pseudo-first order, Pseudo-second order, Elovich and Intra particle diffusion have been investigated using following equations:

$$\log(q_e - q_t) = \log q_e - \frac{k_1}{2.303} t \quad (7)$$

$$\frac{t}{q_t} = \frac{1}{k_2 q_e^2} + \frac{1}{q_e} t \quad (8)$$

$$q_t = \left(\frac{1}{\beta} \right) \ln(\alpha\beta) + \left(\frac{1}{\beta} \right) \ln t \quad (9)$$

$$q_t = k_d t^{1/2} + I \quad (10)$$

where q_e [mg g^{-1}] and q_t refer to the amounts of adsorption at the equilibrium and any time t [min] respectively, k_1 [min^{-1}] and k_2 [$\text{g mg}^{-1} \text{min}^{-1}$] are the adsorption rate constants in the Pseudo-first order adsorption and Pseudo-second order adsorption respectively, k_1 [min^{-1}] can be calculated from the slope of the linear plot of $\log [q_e - q_t]$ versus t and k_2 [$\text{g mg}^{-1} \text{min}^{-1}$] can be obtained from the intercept of the linear

plot of t/q_t versus t (Ahlavanzadeh *et al.* 2010). The parameter of α [$\text{mg g}^{-1}\text{min}^{-1}$] is the initial adsorption rate and β [g mg^{-1}] is the rate desorption constant that can be calculated from the intercept and slope of the linear plot of q_t versus $\ln t$ respectively, k_d [$\text{mg g}^{-1}\text{min}^{-1/2}$] is the intra particle diffusion rate constant [$\text{mg g}^{-1}\text{min}^{-1/2}$] that can be obtained from the slope of the linear plot q_t versus $t^{1/2}$ and l is a constant that gives idea about the thickness of the boundary layer.

3. Results and discussion

3.1. Characterization of HMZ

The results of XRD analysis of HMZ are displayed in Fig. 1. The XRD diffraction pattern shows that clinoptilolite with the empirical formula $((\text{Al}_{6.59}\text{Si}_{29.41}\text{O}_{72})_{28}(\text{H}_2\text{O})_{28}(\text{Na}_{0.52}\text{K}_{2.44}\text{Ca}_{1.48}))$ is 70% of sample. Other components are also found and identified as Ramsdellite (3%), Silicon oxide (8%), Potassium Aluminum Silicate (9%). It indicates the HMZ is mainly composed of clinoptilolite.

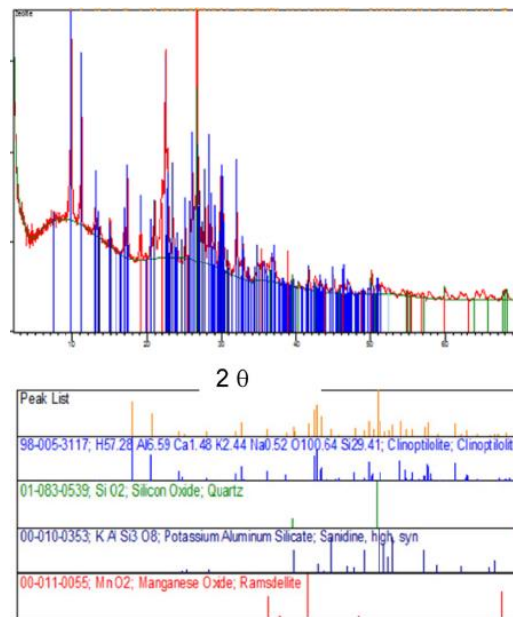


Figure 1. X-ray diffractogram of the HMZ sample

The hypermangan coated on zeolite surface is presented as ramsdellite (manganese (IV) oxide) with chemical formula of MnO_2 . The XRF analysis of the zeolite sample to determine the chemical compositions and characteristics of zeolite used in this study are expressed in Table 2. As is presented, the main components of natural zeolite of Semnan are, SiO_2 and Al_2O_3 . SEM images are very useful in obtaining adsorption details before and after coating.

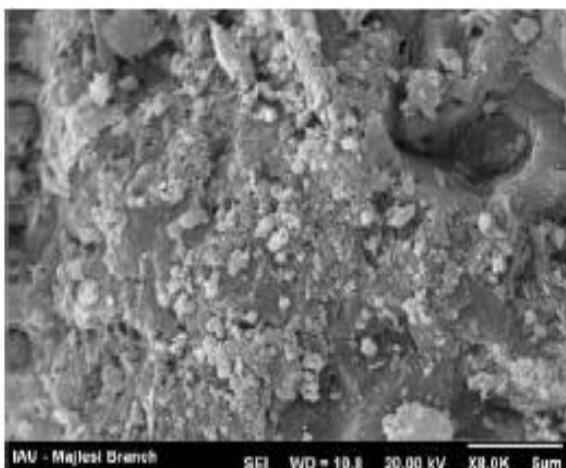
Electron microscope images (SEM, AIS2300C, WD = 8.8) at 20 keV), for raw zeolite and HMZ are shown in Fig. 2. SEM study indicated that the structure of the zeolite changed as a result of coating, as zeolite surface sites were apparently occupied with hypermangan. Electron microscope images of HMZ, represented a grow of hypermangan particles together on the surface of the zeolite and also shows the particles with much rougher surface as evidence of hypermangan particles coating. The FT-IR spectra of HMZ were used to determine the positions of different bands, their assignments and the functional groups in the adsorbent. Fig. 3 exhibits IR spectrums of HMZ.

Table 2. Semi-quantitative XRF analysis results of Semnan zeolite

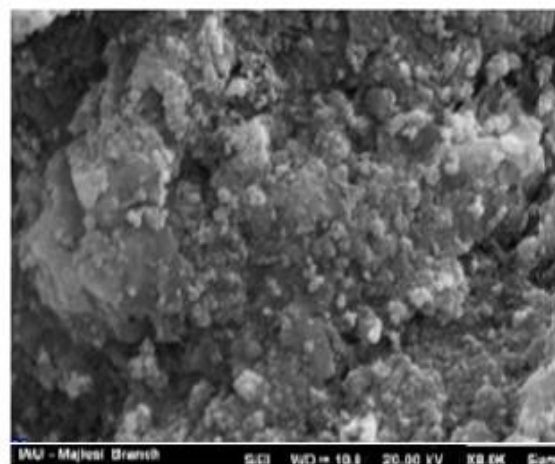
Constituent	Percent
SiO ₂	66.5
Al ₂ O ₃	11.81
Fe ₂ O ₃	1.3
CaO	3.11
MgO	0.72
Na ₂ O	2.01
K ₂ O	3.12
P ₂ O ₅	0.01
MnO	0.04
TiO ₂	0.21
LOI*	12.05

*Loss on ignition

As shown in [Fig. 3], the peaks of at 3,450 and 1,633 cm⁻¹ are due to bending vibration water molecules associated with Na and Ca in the channels of the zeolite. The bonds at 799 and 471 cm⁻¹ are attribute to the presence of O-T-O (T=Si and Al) stretching vibration and the bending vibration mode of T-O, respectively. The peak of 1111 cm⁻¹, is due to asymmetric stretching vibration mode of internal T-O bonds in TO₄ tetrahedra. BET specific surface and total pore volume on the adsorbent were 2.14 m² g⁻¹ and 0.005 cm³ g⁻¹, respectively. Because the specific surface area of HMZ is low, the functional groups likely have a more pronounced role than particle surface area in adsorbing nitrate from liquid. The mean pore diameter was calculated to be 0.64 nm, indicating that HMZ is a micropore adsorbent.



(a)



(b)

Figure 2. SEM images of (a) Raw zeolite, (b) HMZ

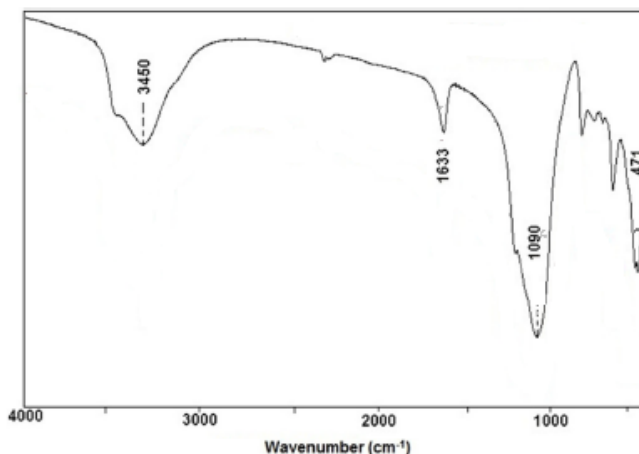


Figure 3. FTIR spectrum of HMZ adsorbent

3.2. Effect of Initial pH

To determine the optimum solution pH, pH was changed from 2-11 at an initial nitrate concentration of 150 mg l⁻¹ and an adsorbent dosage of 0.1 g of HMZ per 100 ml of solution. As presented in Fig. 4, adsorption of nitrate onto HMZ varied with the initial pH of solution, so it is obvious that pH plays a significant role in the adsorption process. It may be due to pH influence on the surface properties of the adsorbent, surface charge of the adsorbent and ionization/dissociation of the adsorbate molecule.

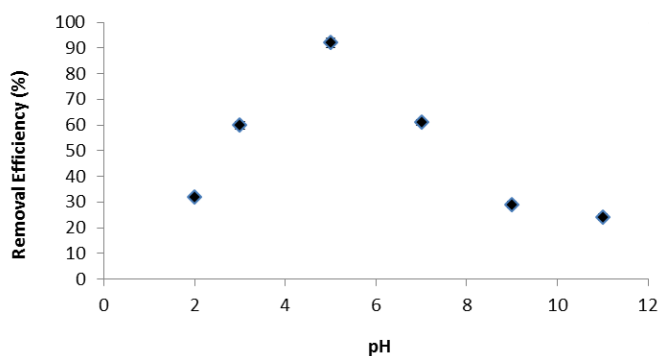


Figure 4. Effect of pH on the adsorption of nitrate onto HMZ ($C_0=150$ mg L⁻¹, $t=60$ min; HMZ dosage = 2 g L⁻¹, $T=25^\circ\text{C}$).

The maximum removal efficiency of the HMZ was observed at a pH of 5.0. According to the researches carried out by other researchers the optimum pH is related to pH_{zpc} ($\text{pH}_{\text{zero point charge}}$) which at this pH, surface charge is neutral and at pH levels lower than pH_{zpc} surface charge is positive, while at pH levels higher than pH_{zpc} surface charge is negative. Nitrate adsorption was found to increase with a decrease in the pH of the solution, because at pH levels with a positive charge, the anions of nitrate can be attracted to the surface of the HMZ having a negative surface charge and can increase the efficiency (decrease in the pH of the solution resulted in more protons being available to protonate the HMZ) (Aguilar *et al.*, 2005). In this study, the isoelectric point of the HMZ was determined to be 6.2 (pH_{zpc}). At a pH levels below 6.2, the surface of the HMZ is positively

charged that it resulted increased electrostatic interactions between negatively charged nitrate group and positively charged HMZ surface. With increasing pH to levels above pH_{zpc} , the number of negatively charged sites increase and the number of positively charged sites decrease. This does not favor the adsorption of anionic nitrate due to electrostatic repulsion. Furthermore, in an alkaline medium, a decrease in removal efficiency is due to the competition of OH^- ions with anionic nitrate for adsorption onto the HMZ. Yanhui *et al.*, used cetylpyridinium bromide (CPB) modified zeolite as adsorbent for removal of nitrate from aqueous solution. They are presented that pH 6.0 is suitable for removal of nitrate by modified zeolite (Yanhui *et al.*, 2011). In other research, Aghaii *et al.*, used modified UZM-5 as adsorbent for nitrate removal from aqueous solution. It be seen that the adsorption of nitrate on adsorbent is clearly pH dependent. The maximum adsorption of nitrate was obtained at pH 7.0 and in both acidic and alkaline range (3–5 and 9–11, respectively) the maximum amount of nitrate adsorption per mass of adsorbent was strongly reduced (Aghaii *et al.*, 2013).

3.3. Influence of HMZ Dosage

The mass of adsorbent can significantly affect adsorption efficiency due to increase in surface area and extension the greater number of exchangeable sites available for interaction with nitrate ions. The effect of HMZ dosage on nitrate removal was investigated at an optimum pH 5.0, under the conditions given in Table 1. As presented in Fig. 5, removal efficiency of nitrate increased with increasing HMZ dosage; as removal percentages of nitrate were obtained 48 % and 92 % for 0.1 and 2 g l⁻¹ of HMZ dosage, respectively. The removal efficiency remained almost unchanged thereafter. It is can be attributed to increase in surface area and available adsorption sites that resulted to high adsorption of nitrate ions onto HMZ. Achievement of a high nitrate removal percentage with a relatively low adsorbent dose indicates the high affinity and suitability of HMZ for removal of nitrate from wastewater.

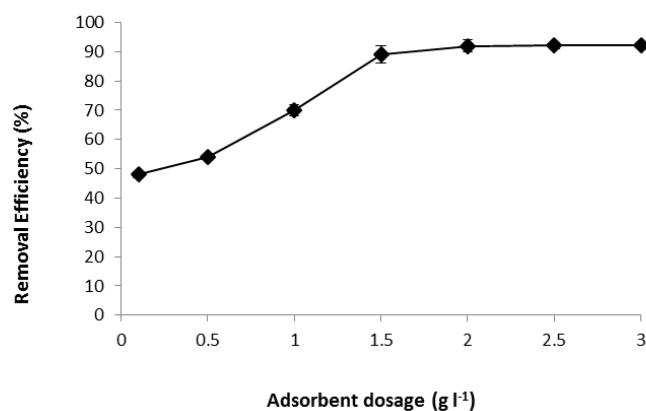


Figure 5. Influence of HMZ dose (0.1–2.5) on nitrate removal by HMZ (pH 5.0, $NO_3^- = 150 \text{ mgL}^{-1}$, contact time = 60 min).

3.3. Equilibrium Adsorption Isotherm

The equilibrium adsorption isotherm describes the relationship of the concentration of an adsorbate between two separate phases at equilibrium at a constant temperature, and this is an important step in finding a suitable model that can be used in the design of adsorption systems (Khorramfar *et al.*, 2009).

The equation parameters of these models often characterize the adsorption mechanism, surface properties and affinity of the adsorbent. In this study, the adsorption of nitrate from its aqueous solution by HMZ was investigated with four of the most used isotherm models (Langmuir, Freundlich, Temkin and (D-R)). The values of related to Isotherm models are summarized in Table 3.

Table 3. Isotherm parameters for nitrate adsorption onto HMZ

Langmuir	
q_m [mg g ⁻¹]	6.7
b [l mg ⁻¹]	1.42
R_L	0.04
R^2	0.995
Freundlich	
K_F [mg g ⁻¹]	37.7
n	0.22
R^2	0.803
Temkin	
B [kJ mol ⁻¹]	21.87
k_t [l mg ⁻¹]	1.47
R^2	0.832
D-R	
q_m [mg g ⁻¹]	7.5
K_{DR} [mg ² KJ ⁻¹]	21.87
E [KJ mg ⁻¹]	0.15
R^2	0.954

In the Langmuir isotherm model, it is assumed that all active sites have equal affinity for the sorbate, and this leads to monolayer coverage of the adsorbate at specific homogeneous sites on the outer surface of the adsorbent, therefore molecule or ion occupies the adsorption site, no further adsorption can take place. It is no dependency of molecule to the neighboring sites which is considered as monolayer adsorption. Maximum uptake capacity of unmodified zeolite was determined with the Langmuir model (3.7 mg g⁻¹) and compared with the maximum uptake capacity of nitrate on the HMZ (6.7 mg g⁻¹), that it can be due to increase of active surfaces of modified adsorbent that it leads to increase of nitrate removal using permanganate modification. Yanhui *et al.* reached to maximum uptake capacity of 9.35 to 9.68 for different temperature, in removal of nitrate by modified zeolite with cetylpyridinium bromide (Yanhui *et al.*, 2011). In research of Aghaii *et al.*, the maximum monolayer sorption capacity of SMU for nitrate removal was found to be 18.62 mg g⁻¹ at 298 K (Aghaii *et al.*, 2013).

The value of R_L describes the adsorption characteristics as follows:

$R_L = 1$ linear.

$R_L = 0$ irreversible.

$R_L > 1$ unfavorable.

$0 < R_L < 1$ favorable.

Since the value of R_L is between 0 and 1, therefore adsorption of nitrate on HMZ is favorable (because of $R_L=0.04$).

The Freundlich isotherm model is derived by assuming a heterogeneous surface. It is not limited to the formation of monolayer. This model is an empirical isotherm which describes non-ideal adsorption on heterogeneous surfaces and reversible adsorption. The K_F value indicates the adsorption capacity of the adsorbent that with increasing it, adsorption capacity increases. The value of n for HMZ was between 0 and 1 (0.22). This shows that nitrate adsorption onto HMZ is beneficial adsorption.

Sudipta *et al.*, in their research (removal of nitrate from aqueous solutions by chitosan hydrogel beads) said that RL value calculated using $C_o = 1000 \text{ mg l}^{-1}$ is well within the defined range (0.07) and indicate the acceptability of the process (Sudipta *et al.*, 2009).

D-R isotherm determines a high degree of regularity, adsorption type and the mechanism.

The mean free energy of adsorption [E] can be written as:

$$E=1/[2K_{DR}]^{0.5} \quad (6)$$

The amount of E is used to determine the mechanism of the adsorption process. For instance, if the value of E is between 8 and 16 kJ mol^{-1} , the adsorption process occurs through a chemical mechanism and if the value of E is less than 8 kJ mol^{-1} , the adsorption process occurs through a physical mechanism. For the adsorption of nitrate onto HMZ, the value of E was 0.15 kJ mol^{-1} , which indicates the adsorption of nitrate onto the HMZ occurs through a physical mechanism. Based on Table 2, values of the correlation coefficients (R^2) were 0.995, 0.803, 0.832 and 0.954 for Langmuir, Freundlich, Temkin and D-R models respectively. The high correlation coefficient value obtained from the Langmuir isotherm equation (0.995), indicates that the equilibrium data fit well with Langmuir model. It is the most common isotherm equation to use due to its simplicity and its ability to fit a variety of adsorption data. It is based on four assumptions:

1. All of the adsorption sites are equivalent and each site can only accommodate one molecule.
2. The surface is energetically homogeneous and adsorbed molecules do not interact.
3. There are no phase transitions.
4. At the maximum adsorption, only a monolayer is formed. Adsorption only occurs on localized sites on the surface, not with other adsorbents.

3.4. Kinetic Study

The effect of time on nitrate sorption efficiency was evaluated. As presented in Fig. 6, the time required to reach an equilibrium state was achieved in 60 min. Therefore the shaking time was fixed in 60 min. Adsorption is a surface phenomenon, that is related to surface area per unit weight and accessibility to pore of the adsorbent. Adsorption kinetics are important for evaluating the efficacy of adsorption and identify the adsorption mechanism. Kinetics of adsorption described chemical reaction rate and potential rate controlling steps. The kinetic behavior of this process was studied at pH 5.0 and 25 °C in shaking time 5 to 60 min. The experimental data were fitted to four kinetics models including Pseudo-first order, Pseudo-second order, Elovich and Intra particle diffusion. The results of kinetic studies are shown in Table 4.

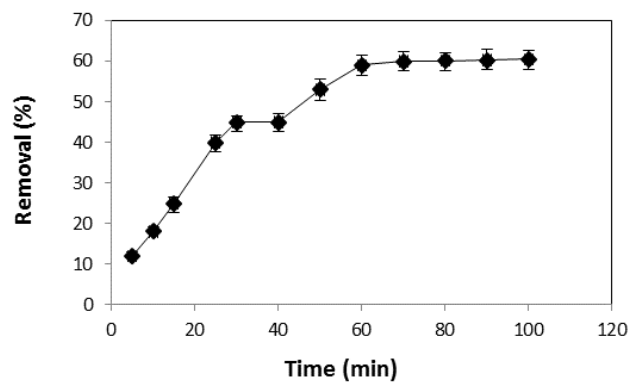


Figure 6. Effect of contact time on the adsorption of nitrate onto HMZ ($C_o=150 \text{ mg l}^{-1}$, HMZ dosage = 2g l^{-1} , $T=25 \text{ }^\circ\text{C}$)

The parameters of kinetic models are presented in Table 4. The models were evaluated based on correlation coefficient, R^2 and difference between the q_e (theor) value with q_e (exp). According to Table 4, the Pseudo-first-order kinetic model has higher correlation coefficient ($R^2=0.971$) than the others as it is observed a little difference between $q_{e, \text{exp}}$ and $q_{e, \text{cal}}$ and the R^2 values are close to 1.

Sudipta *et al.*, in their research about removal of nitrate from aqueous solutions by chitosan hydrogel beads, said, the line for Pseudo-second-order model has higher correlation coefficients ($R^2= 0.999$) compared to the correlation coefficient ($R^2= 0.988$) obtained from the linear plot of the Pseudo-first-order rate model. (Sudipta *et al.*, 2009).

The validity of the Pseudo-first and second order models was assessed by calculating the standard deviation between model-predicted and experimental adsorption capacities. As shown in Table 4, the values of Δq for all three concentrations were very low for the Pseudo-first order model in comparison to those for the Pseudo-second order model, confirming the applicability of the former. So, the adsorption behavior can be interpreted very well by this kinetic model over the whole range of contact time. The Intra particle diffusion model is to elucidate the diffusion mechanism. In many adsorption processes an Intra particle diffusion model, is the rate limiting step [if plot of q_t versus $T^{1/2}$ be straight line]. Also according to this model, if multi linear plots involve various steps, then two or more steps influence the adsorption process.

Table 4. Kinetic parameters for nitrate adsorption onto HMZ

C_0 [mg L ⁻¹]	100	150	200	250	300	
$q_{e, \text{exp}}$ [mg g ⁻¹]	5.7	7.8	18	24	35	
Pseudo-first- order	$q_{e, \text{cal}}$ [mg g ⁻¹]	4.3	7.29	16.5	22.8	33
	k1 [min ⁻¹]	0.1	0.029	0.011	0.0005	0.0006
	R^2	0.98	0.991	0.978	0.967	0.985
	Δq (%)	2	1.2	2.2	2.4	2.1
Pseudo- second-order	$q_{e, \text{cal}}$ [mg g ⁻¹]	11.8	14.2	22.3	27	30.2
	k2 [g mg ⁻¹ min ⁻¹]	0.035	0.019	0.011	0.011	0.009
	R^2	0.964	0.953	0.941	0.955	0.938
	Δq (%)	48	46	40	35	50
Elovich	α [mg g ⁻¹ min ⁻¹]	5.5	8.3	11	15	13.5
	β [g mg ⁻¹]	7.2	6.5	5.5	4.5	3.5
	R^2	0.921	0.964	0.923	0.954	0.968
Intra- particle diffusion	k_d [mg g ⁻¹ min ^{-1/2}]	1.2	2.5	3.8	5.9	9.8
	l [mg g ⁻¹]	11.5	18.9	22.8	32.1	34.2
	R^2	0.889	0.927	0.954	0.925	0.948

The kinetic data were analyzed by an Intra particle diffusion model, which often is the rate limiting step in many adsorption processes. In this model, if plot of q_t versus $T^{1/2}$ be straight line, the adsorption process is controlled by intra particle diffusion. Also according to Intra particle model, if multi linear plots involve various step, then two or more steps influence the adsorption process. The plot of q_t versus $T^{1/2}$ was straight line. The linearity of the plots illustrates that adsorption process may be controlled by Intra particle diffusion that indicates Intra particle diffusion involved in the nitrate adsorption onto HMZ, but it is not the sole rate controlling step.

4. Conclusions

In this study, the adsorption of nitrate onto HMZ adsorbent was investigated in equilibrium and kinetics. It was found that Langmuir isotherm model fitted best the equilibrium data and the maximum adsorption capacity 6.7 mg g^{-1} for nitrate was obtained. Also, the correlation coefficient greater than 0.97 indicated the applicability of Pseudo-first order adsorption model for nitrate adsorption onto HMZ. The clinoptilolite is 70% of HMZ. Intra particle diffusion is sole rate controlling factor and the process may be controlled by intra particle diffusion. The investigation shows favorable adsorption site for nitrate on the surface of HMZ adsorption and shows that HMZ is a promising adsorbent for the removal of nitrate from aqueous solution.

References

- Aghaii M.D., Pakizeh M. and Ahmadpour A. (2013), Synthesis and characterization of modified UZM-5 as adsorbent for nitrate removal from aqueous solution, *Separation and Purification Technology*, **113**, 24–32.
- Aguilar M.I., Saes J., Lorene M., Solar A., Ortuno J.F., Meseguer V. and Fuentes A. (2005), Improvement of coagulation-flocculation process using anionic polyacrylamide as coagulant aid, *Chemosphere*, **58**, 47-56.
- Al Ghouti M.A., Al Degs Y.S., Khraisheh M.A.M., Ahmad M.N. and Allen S.J. (2009), Mechanisms and chemistry of dye adsorption on manganese oxides-modified diatomite, *J. Environ. Manag.*, **90**, 3520-3527.
- Andalib M., Nakhla G. and Zhu J. (2012), High-rate biological nutrient removal from high-strength wastewater using anaerobic-circulating fluidized bed bioreactor (A-CFBBR), *Bioresour. Technol.*, **118**, 526-535.
- APHA, (2005). Standard Methods for the Examination of Water and Wastewater, 21st Ed, American Public Health Association, Washington.
- Benyoucef N., Cheikh A., Drouiche N., Lounici H., Mameri N. and Abdi N. (2013), Denitrification of groundwater using Brewer's spent grain as biofilter media, *Ecol. Eng.*, **52**, 70-74.
- Bravo R., Segovia E., Guerrero L., Montalvo S., Barahona A. and Borja R. (2013), Total ammoniacal nitrogen biofiltration of wastewaters from aquaculture systems using *Macrocystis* spp, *J. Environ. Sci. Health*, **48**, 400-407.
- Cheikh A., Yala A., Drouiche N., Abdi N., Lounici H. and Mameri N. (2013), Denitrification of water in packed beds using bacterial biomass immobilized on waste plastics as supports, *Ecol. Eng.*, **53**, 329–334.
- Dong L., Zhu Z., Ma H., Qiu Y. and Zhao J. (2010), Simultaneous sorption of lead and cadmium on MnO_2 -loaded resin, *J. Environ. Sci.*, **22**, 225-229.
- Gupta V.K., Agarwal S. and Saleh T.A. (2011), Synthesis and characterization of alumina-coated carbon nanotubes and their application for lead removal, *J. Hazard. Mater.*, **185**, 17–23.
- Gupta S.S. and Bhattacharyya K.G. (2008), Immobilization of Pb(II), Cd(II) and Ni(II) ions on kaolinite and montmorillonite surfaces from aqueous medium, *J. Environ. Manag.*, **87**, 46-58.
- Jiang T., Zhang H., Qiang H., Yang F., Xu X. and Du H. (2013), Start-up of the anammox process and membrane fouling analysis in a novel rotating membrane bioreactor, *Desalination*, **311**, 46-53.
- Hajdu I., Bodnár M., Csikós Z., Wei S., Daróczy L., Kovács B., Győri Z., Tamás J. and Borbély J. (2012), Combined nano-membrane technology for removal of lead ions, *J. Membr. Sci.*, **409**, 44-53.
- Han R.H., Zou W., Zhang Z.P., Shi J. and Yang J.J. (2006), Removal of copper(II) and lead(II) from aqueous solution by manganese oxide coated sand: I. Characterization and kinetic study, *J. Hazard. Mater.*, **137**, 384-395.
- Han R.P., Zou W.H., Li H.K., Li Y.H. and Shi J. (2006), Copper(II) and lead(II) removal from aqueous solution in fixed-bed columns by manganese oxide coated zeolite, *J. Hazard. Mater.*, **137**, 934-942.
- Khorramfar S., Mahmoodi N.M., Arami M. and Gharanjig K. (2009), Dye Removal from Colored Textile Wastewater Using *Tamarindus Indica* Hull: Isotherm and Kinetics Study, *Journal of Color Science Technology*, **3**, 81-88.
- Malekian R., Abedi-Koupai J., Eslamian S.S., Mousavi S.F., Abbaspour K.C. and Afyuni M. (2011), Ion-exchange process for ammonium removal and release using natural Iranian zeolite, *Appl. Clay Sci.*, **51**, 323-329.

- Montalvo S., Olivares P., Guerrero L. and Borja R. (2011), Nitrogen and phosphorus removal using a novel integrated system of natural zeolite and lime, *J. Environ. Sci. Health*, **47**, 1385-1391.
- Ngah W.W. and Hanafiah M. (2008), Adsorption of copper on rubber (*Hevea brasiliensis*) leaf powder: Kinetic, equilibrium and thermodynamic studies, *Biochemical Engineering Journal*, **39**, 521-530.
- Rezakazemi M., Shirazian S. and Ashrafizadeh S.N. (2012), Simulation of ammonia removal from industrial wastewater streams by means of a hollow-fiber membrane contactor, *Desalination*, **285**, 383-392.
- Sudipta C. and Seung H. W. (2009), The removal of nitrate from aqueous solutions by chitosan hydrogel beads, *Journal of Hazardous Materials*, **164**, 1012-1018
- Yanhui Z., Jianwei L. and Zhiliang Z. (2011), Removal of nitrate from aqueous solution using cetylpyridinium bromide (CPB) modified zeolite as adsorbent, *Journal of Hazardous Materials*, **186**, 1972-1978
- Yu R., Geng J., Ren H., Wang Y. and Xu K. (2013), Struvite pyrolysate recycling combined with dry pyrolysis for ammonium removal from wastewater, *Bioresour. Technol*, **132**, 154-159.
- Zhang T., Ding L., Ren H. and Xiong X. (2009), Ammonium nitrogen removal from coking wastewater by chemical precipitation recycle technology, *Water Res.*, **43**, 5209-5215.
- Zou W., Han R., Chen Z., Jinghua Z. and Shi J. (2006), Kinetic study of adsorption of Cu(II) and Pb(II) from aqueous solutions using manganese oxide coated zeolite in batch mode, *Colloids and Surfaces A: Physicochemical and Engineering Aspects*, **279**, 238-246.